Available online at www.sciencedirect.com
SCIENCE DIRECT®
Journal of Sound and Vibration 278 (2004) 1131–1146
JOURNAL OF SOUND AND VIBRATION
www.elsevier.com/locate/jsvi

Vibration analysis of a high-speed spindle under the action of a moving mass

U.C. Gu, C.C. Cheng*

Department of Mechanical Engineering, National Chung Cheng University, Chia-Yi 621, Taiwan

Received 21 October 2002; accepted 27 October 2003

Abstract

The dynamic response of a high-speed spindle subject to a moving mass is studied. The system under investigation consists of a ball screw and a moving nut; both of which are key components of a high-speed feed drive system for a machine tool. The ball screw is modelled as a high-speed rotating shaft using Timoshenko beam theory and the nut is modelled as a moving concentrated mass. The system dynamic equation and the corresponding transient response are obtained through Lagrangian approach and Runge–Kutta method, respectively. Influences of parameters on the transient response of the system such as the mass moving speed, the Rayleigh coefficient and the mass ratio are discussed. Results show that the inertia effect caused by the moving nut influences the deflection in the orthogonal direction of the moving nut much more than that in the transverse direction. The maximum deflection in the orthogonal direction under the moving nut could be several times larger than that under the equivalent force for a short and stubby rotating shaft. Moreover, the moving nut reduces the critical frequencies of the spindle. Therefore, the critical frequencies of a ball screw could be seriously overestimated if the ball screw system is modelled either as a shaft subjected to a moving force or as a shaft alone with the moving nut excluded.

1. Introduction

Dynamic responses of a non-rotating beam subjected to a moving load have been studied by many researchers [1–8]. Applications are mainly related to the prediction of behaviors of railway tracks, bridges, etc. In respect to the vibration characteristics of a rotating shaft subjected to a moving load, reported results are also abundant [9–16]. Katz et al. [9] investigated the dynamic response of rotating shafts based on the respective Euler, Rayleigh and Timoshenko beam models subjected to a constant velocity moving forces using transformation methods. Argento and Scott

*Corresponding author. Tel.: +886-5-2720411-33313; fax: +886-5-2720589.
E-mail address: imeccc@ccu.edu.tw (C.C. Cheng).

0022-460X/$ - see front matter
doi:10.1016/j.jsv.2003.10.034

[10] generalized Katz's results to a rotating beam subjected to an accelerating distributed surface force. Lee [11] investigated the dynamic response of a rotating Timoshenko beam subjected to both axial forces and moving forces. The related problems in the area of deflection- and motion-dependent forces on a rotating shaft are also studied by Argento [12,13] and Huang [14]. An application of this class of problem is found in machining processes where the moving force simulates a tool and the rotating shaft a workpiece. Although the vibration characteristics of a rotating shaft has been investigated extensively, there are still some fundamental issues that remain open and need to be addressed, especially when the rotating shaft is subjected to a moving mass instead of a moving force.

The system under investigation in this paper consists of a ball screw and a nut moving along it, which are the key components of a feed drive system for a machine tool. The focus is on the dynamic response of a high-speed rotating, short ball screw shaft subjected to a high-speed moving nut. The ball screw is modelled as a high-speed rotating shaft and the moving nut as a moving concentrated mass. For a short and stubby rotating shaft, the shear and rotary inertia effects must be captured for an accurate dynamic analysis. Therefore the rotating shaft is modelled based on Timoshenko beam theory.

Equations of motion for a rotating shaft subject to moving loads based on Timoshenko theory can be derived using either Newton's method [9] or Hamilton's principle [11]. Then, the shaft deformation expressed in terms of either an inertia frame [8,10] or a co-ordinate system fixed to the rotating shaft [16] can be determined by using the modal analysis or the assumed mode method or the integral transformation method. The present work formulates a rotating shaft subjected to a moving mass through the energy method and quantifies the differences in vibration responses between a rotating shaft subjected to a moving mass and that subjected to a moving force. In addition, the influences of the inertia effect induced by the moving mass on the whirl speed are also investigated.

2. Formulation

Consider a uniform shaft of length L lying in the x–z plane and rotating at a constant angular velocity Ω as shown in Fig. 1. A concentrated mass M moves with a constant speed v_m along the

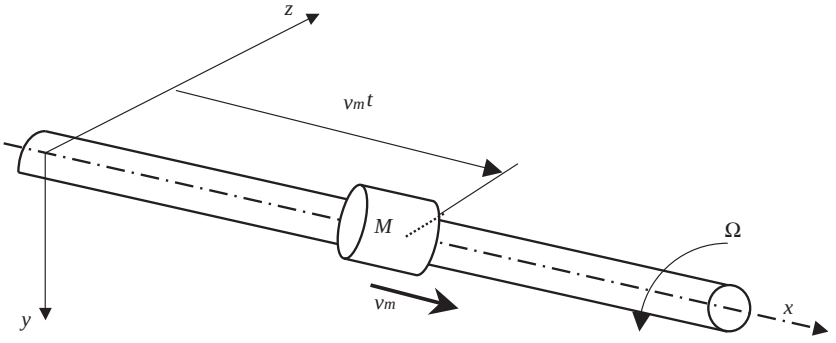

Fig. 1. Geometry of a spinning shaft subjected to a moving mass.

shaft but does not rotate with the shaft. The moving mass is assumed to remain in contact with the shaft during the motion. The shaft has a cross-sectional area A, second moment of area I, cross-sectional shape factor κ, Young's modulus E, shear modulus G and density ρ. The deformed beam is described by the transverse translations $V(x,t)$ and $W(x,t)$ in the y and z directions and small rotations $B(x,t)$ and $\Gamma(x,t)$ about the y- and z-axis, respectively. Based on the Timoshenko beam theory, the translations (V, W) consist of a contribution (V_b, W_b) due to bending and a contribution (V_s, W_s) due to transverse shear deformation. The relationships between variables of the translation and rotation are given as follows:

$$V(x,t) = V_b(x,t) + V_s(x,t), \quad W(x,t) = W_b(x,t) + W_s(x,t), \tag{1a}$$

$$B(x,t) = -\frac{\partial W_b(x,t)}{\partial x}, \quad \Gamma(x,t) = \frac{\partial V_b(x,t)}{\partial x}. \tag{1b}$$

Note that rotations B and Γ are only related to the bending deformations W_b and V_b, respectively. Using the assumed mode method, V, W, B and Γ can be expressed as

$$V(x,t) = \sum_{i=1}^{n} v_i(t)\phi_i(x), \quad W(x,t) = \sum_{i=1}^{n} w_i(t)\phi_i(x), \tag{2a}$$

$$B(x,t) = \sum_{i=1}^{n} p_i(t)\varphi_i(x), \quad \Gamma(x,t) = \sum_{i=1}^{n} q_i(t)\varphi_i(x), \tag{2b}$$

where n is the mode number, $\phi_i(x)$ and $\varphi_i(x)$ are shape functions that satisfy the corresponding shaft boundary conditions; $v_i(t)$, $w_i(t)$, $p_i(t)$ and $q_i(t)$ are the respective modal displacements. For a shaft with simply supported at both ends as an example, the shape functions can be expressed as

$$\phi_i(x) = \sqrt{2}\sin\frac{i\pi x}{L} \tag{3a}$$

and

$$\varphi_i(x) = \sqrt{2}\cos\frac{i\pi x}{L}. \tag{3b}$$

The potential energy U_s of a uniform shaft which consists of strain energies of bending and shear is given by

$$U_s = \frac{1}{2}\int_0^L EI\{(V_b'')^2 + (W_b'')^2\}\,\mathrm{d}x + \frac{1}{2}\int_0^L \kappa AG\{(V_s')^2 + (W_s')^2\}\,\mathrm{d}x, \tag{4}$$

where the superscript "$'$" indicates differentiation with respect to x. Eq. (4) can be rewritten in terms of V, W, B and Γ as

$$U_s = \frac{1}{2}\int_0^L EI\{(\Gamma')^2 + (B')^2\}\,\mathrm{d}x + \frac{1}{2}\int_0^L \kappa AG\{(V')^2 + (W')^2 + \Gamma^2 + B^2 - 2\Gamma V' + 2BW\}\,\mathrm{d}x. \tag{5}$$

The kinetic energy T, including contributions from the shaft rotating at a constant speed Ω and the mass moving at a constant speed v_m, is expressed as

$$T = T_s + T_M, \tag{6}$$

where

$$T_s = \frac{1}{2}\int_0^L \rho A\{\dot{V}^2 + \dot{W}^2\}\,\mathrm{d}x + \frac{1}{2}\int_0^L \rho I\{\dot{B}^2 + \dot{\Gamma}^2\}\,\mathrm{d}x - \tfrac{1}{2}\Omega(2\rho I)\int_0^L \{\dot{\Gamma}B - \dot{B}\Gamma\}\,\mathrm{d}x + \tfrac{1}{2}\Omega^2\int_0^L 2\rho I\,\mathrm{d}x, \tag{7}$$

$$T_M = \tfrac{1}{2}M\left[v_m^2 + \left(\frac{\partial V}{\partial t} + v_m\frac{\partial V}{\partial x}\right)^2 + \left(\frac{\partial W}{\partial t} + v_m\frac{\partial W}{\partial x}\right)^2\right]\Bigg|_{x=v_m t}. \tag{8}$$

The superscript "." in Eq. (7) denotes differentiation with respect to time; and T_s and T_M are the kinetic energies for the rotating shaft and the moving mass, respectively. The second and third terms of the kinetic energy of the moving mass is due to the transverse components of the velocity of the mass caused by the deflection of the shaft as well as the horizontal motion of the mass. The virtual work $\delta \mathrm{W}_g$ of the gravitational force on the system is

$$\delta \mathrm{W}_g = Mg\delta V|_{x=v_m t}, \tag{9}$$

where $\delta V|_{x=v_m t}$ is the virtual displacement of V evaluated at $x=v_m t$. Upon substituting Eqs. (4)–(9) into Lagrange's equation [17], the equations of motion for the system is given as

$$(\rho A\mathbf{M} + M\mathbf{B})\ddot{\mathbf{v}} + 2Mv_m\mathbf{A}\dot{\mathbf{v}} + (\kappa AG\mathbf{H} + Mv_m^2\mathbf{C})\mathbf{v} - \kappa AG\mathbf{E}^{\mathrm{T}}\mathbf{q} = mg\mathbf{a}, \tag{10}$$

$$(\rho A\mathbf{M} + M\mathbf{B})\ddot{\mathbf{w}} + 2Mv_m\mathbf{A}\dot{\mathbf{w}} + (\kappa AG\mathbf{H} + Mv_m^2\mathbf{C})\mathbf{w} - \kappa AG\mathbf{E}^{\mathrm{T}}\mathbf{p} = \mathbf{0}, \tag{11}$$

$$\rho I\mathbf{S}\ddot{\mathbf{p}} + 2\Omega\rho I\mathbf{S}\dot{\mathbf{q}} + EI\mathbf{K}\mathbf{p} + \kappa AG\mathbf{S}\mathbf{p} + \kappa AGE\mathbf{w} = \mathbf{0}, \tag{12}$$

$$\rho I\mathbf{S}\ddot{\mathbf{q}} + 2\Omega\rho I\mathbf{S}\dot{\mathbf{p}} + EI\mathbf{K}\mathbf{q} + \kappa AG\mathbf{S}\mathbf{q} - \kappa AG\mathbf{E}\mathbf{v} = \mathbf{0}, \tag{13}$$

where

$$\mathbf{v} = \{v_1, v_2, \ldots, v_n\}^{\mathrm{T}}, \quad \mathbf{w} = \{w_1, w_2, \ldots, w_n\}^{\mathrm{T}}, \quad \mathbf{p} = \{p_1, p_2, \ldots, p_n\}^{\mathrm{T}}, \quad \mathbf{q} = \{q_1, q_2, \ldots, q_n\}^{\mathrm{T}},$$

$$\mathbf{M} = \{m_{ij}\}, \quad m_{ij} = \int_0^L \phi_i\phi_j\,\mathrm{d}x, \quad \mathbf{S} = \{s_{ij}\}, \quad s_{ij} = \int \varphi_i\varphi_j\,\mathrm{d}x,$$

$$\mathbf{K} = \{k_{ij}\}, \quad k_{ij} = \int_0^L \varphi_i'\varphi_j'\,\mathrm{d}x, \quad \mathbf{H} = \{h_{ij}\}, \quad h_{ij} = \int_0^L \phi_i'\phi_j'\,\mathrm{d}x, \quad \mathbf{E} = \{e_{ij}\}, \quad e_{ij} = \int_0^L \varphi_i\phi_j'\,\mathrm{d}x,$$

$$\mathbf{a} = \{a_i\}, \quad a_i = \phi_i(x = v_m t), \quad C = \{c_{ij}\}, \quad c_{ij} = \phi_i'(x = v_m t)\phi_j'(x = v_m t),$$

$$\mathbf{A} = \{A_{ij}\}, \quad A_{ij} = \tfrac{1}{2}(\phi_i(x = v_m t)\phi_j'(x = v_m t) - \phi_i'(x = v_m t)\phi_j(x = v_m t)),$$

$$\mathbf{B} = \{b_{ij}\}, \quad b_{ij} = \phi_i(x = v_m t)\phi_j(x = v_m t). \tag{14a–v}$$

Note that matrices and vectors are represented by boldfaced letters. The terms on the left-hand side in Eqs. (10)–(13) include the flexural stiffness, the transverse shear, the rotary inertia, the gyroscopic effect, the lateral inertia, the coupling between transverse shear and the gyroscopic effects and the coupling between transverse shear and the rotary inertia. One can express Eqs. (10)–(13) using a matrix equation as

$$\bar{\mathbf{M}}\ddot{\mathbf{Q}} + \bar{\mathbf{C}}\dot{\mathbf{Q}} + \bar{\mathbf{K}}\mathbf{Q} = \bar{\mathbf{F}}, \tag{15}$$

where

$$\mathbf{Q} = \{v_1, v_2, \ldots, v_n, w_1, w_2, \ldots, w_n, p_1, p_2, \ldots, p_n, q_1, q_2, \ldots, q_n\}^{\mathrm{T}},$$

$$\bar{\mathbf{F}} = \{Mg\mathbf{a}, \mathbf{0}, \mathbf{0}, \mathbf{0}\}^{\mathrm{T}},$$

$$\bar{\mathbf{M}} = \begin{bmatrix} \rho A\mathbf{M} + M\mathbf{B} & 0 & 0 & 0 \\ 0 & \rho A\mathbf{M} + M\mathbf{B} & 0 & 0 \\ 0 & 0 & \rho I\mathbf{S} & 0 \\ 0 & 0 & 0 & \rho I\mathbf{S} \end{bmatrix},$$

$$\bar{\mathbf{C}} = \begin{bmatrix} 2Mv_m\mathbf{A} & 0 & 0 & 0 \\ 0 & 2Mv_m\mathbf{A} & 0 & 0 \\ 0 & 0 & 0 & 2\rho I\Omega\mathbf{S} \\ 0 & 0 & -2\rho I\Omega\mathbf{S} & 0 \end{bmatrix},$$

$$\bar{\mathbf{K}} = \begin{bmatrix} \kappa AG\mathbf{H} - Mv_m^2\mathbf{C} & 0 & 0 & -\kappa AG\mathbf{E}^{\mathrm{T}} \\ 0 & \kappa AG\mathbf{H} - Mv_m^2\mathbf{C} & \kappa AG\mathbf{E}^{\mathrm{T}} & 0 \\ 0 & \kappa AG\mathbf{E} & 0 & 0 \\ -\kappa AG\mathbf{E} & 0 & 0 & EI\mathbf{K} + \kappa AG\mathbf{S} \end{bmatrix}. \tag{16a–e}$$

If the moving mass is replaced by a moving force, the equation of motion is expressed as

$$\bar{\mathbf{M}}_f\ddot{\mathbf{Q}} + \bar{\mathbf{C}}_f\dot{\mathbf{Q}} + \bar{\mathbf{K}}_f\mathbf{Q} = \bar{\mathbf{F}}, \tag{17}$$

where

$$\bar{\mathbf{F}} = \{Mg\mathbf{a}, \mathbf{0}, \mathbf{0}, \mathbf{0}\}^{\mathrm{T}},$$

$$\bar{\mathbf{M}}_f = \begin{bmatrix} \rho A\mathbf{M} & 0 & 0 & 0 \\ 0 & \rho A\mathbf{M} & 0 & 0 \\ 0 & 0 & \rho I\mathbf{S} & 0 \\ 0 & 0 & 0 & \rho I\mathbf{S} \end{bmatrix}, \quad \bar{\mathbf{C}}_f = \begin{bmatrix} 0 & 0 & 0 & 0 \\ 0 & 0 & 0 & 0 \\ 0 & 0 & 0 & 2\rho I\Omega\mathbf{S} \\ 0 & 0 & -2\rho I\Omega\mathbf{S} & 0 \end{bmatrix},$$

$$\bar{\mathbf{K}}_f = \begin{bmatrix} \kappa AG\mathbf{H} & 0 & 0 & -\kappa AG\mathbf{E}^{\mathrm{T}} \\ 0 & \kappa AG\mathbf{H} & \kappa AG\mathbf{E}^{\mathrm{T}} & 0 \\ 0 & \kappa AG\mathbf{E} & 0 & 0 \\ -\kappa AG\mathbf{E} & 0 & 0 & EI\mathbf{K} + \kappa AG\mathbf{S} \end{bmatrix}. \tag{18a–d}$$

Comparing Eqs. (16) with (18), the differences in equation of motions between a rotating shaft subjected to a moving mass and that subjected to a moving force are $M\mathbf{B}\ddot{\mathbf{v}}, M\mathbf{B}\ddot{\mathbf{w}}$, $2Mv_m\mathbf{A}\dot{\mathbf{v}}, 2Mv_m\mathbf{A}\dot{\mathbf{w}}, -Mv_m^2\mathbf{C}\mathbf{v}$ and $-Mv_m^2\mathbf{C}\mathbf{w}$, which characterize the inertia effect caused by the moving concentrated mass. The first two terms represent the inertia forces in the tangential direction, the third and forth terms are the Coriolis forces and the last two terms are the centripetal forces.

As an alternative, one can derive the equation of motion for the same rotating shaft subjected to a moving mass using Hamilton's principle as shown in the appendix. Instead of a system of

ordinary differential equations derived previously using assumed-mode method, the equations of motion consists of two partial differential equations, one is designated for the transverse translations $V(x,t)$ and the other for $W(x,t)$. The equation of motion denotes the force equilibrium and each term represents a distributed force caused by the transverse shear, the gyroscopic effect, the lateral inertia, the rotary inertia and couplings induced from the moving mass. Consequently, the enhanced couplings among the transverse shear, the gyroscopic effect, the lateral inertia and the rotary inertia arising from the moving mass can be identified explicitly as described in the appendix.

The numerical scheme of the system is obtained by introducing state vectors into the equations of motion and hence reducing these equations to a set of first order state equations with specified initial conditions that are solved by using the Runge–Kutta method [18].

3. Non-dimensionalization

The dimensionless shaft deflections, moving mass speed, mass size, shaft rotational speed, and Rayleigh beam coefficient are defined as follows:

$$V/V_s, \quad W/V_s, \quad \alpha = v_m/v_{cr}, \quad \bar{\Omega} = \Omega/\omega_{1EB}, \quad \beta = \frac{\pi r_0}{L}, \quad \bar{m} = \frac{M}{\rho A L}, \tag{19}$$

where $v_{cr} = (\pi/L)\sqrt{EI/\rho A}$ is the fundamental critical speed of a pined–pined, non-rotating Euler–Bernoulli beam, β is the Rayleigh beam coefficient, r_0 is the radius of gyration, ω_{1EB} and $V_s = MgL^3/48EI$ are the first natural frequency and the static deflection at midspan of a pined–pined Euler–Bernoulli beam. The non-dimensional parameters related to the mass moving speed, mass size, the Rayleigh coefficient and shaft rotating speed are $0 \leqslant \alpha \leqslant 1.5$, $0.1 \leqslant \bar{m} \leqslant 0.4$, $\beta \leqslant 0.3$, and $\bar{\Omega} \leqslant 2.5$, respectively, which covers most of the high-speed, short and stubby rotating shaft in engineering application. In order to evaluate the dynamic response, several parameters must be specified to illustrate some features of the theoretical results. A rotating steel shaft with pined–pined boundary conditions is chosen and the corresponding parameters are: $\rho = 7700\,\mathrm{kg/m^3}$, $\kappa = 0.9$, $E = 207\,\mathrm{GPa}$, $G = 77.6\,\mathrm{GPa}$, $L = 1\,\mathrm{m}$ and $g = 9.81\,\mathrm{m/s^2}$, which are the same shaft parameters and material properties defined in Ref. [11] for the purpose of comparison. Numerical results were computed using 10 modes in order to satisfy the criterion of convergence.

4. Numerical results and discussion

In this paper, of interest are the differences in the maximum shaft deflection caused by a moving mass and that by an equivalent moving force to see the influence of inertia effect caused by the moving mass on a high-speed rotating shaft response. Numerical results have been divided into three sections to investigate the effects of moving mass speed, moving mass size and the shaft diameter on the shaft response, respectively. Also, a study of influences of the moving mass on the critical speed prediction is included.

4.1. Influences of the shaft diameter and mass moving speed on the shaft response

The normalized deflections V/V_s, W/V_s of a simply supported beam rotating at the speed $\bar{\Omega} = 2.5$ under a moving mass, $\bar{m} = 0.2$ are plotted in Fig. 2 for $\alpha = 0.1$ and Fig. 3 for $\alpha = 1.5$, respectively. In order to aid the comparison, deflections for the same beam subjected to an equivalent moving force with amplitude that is equal to Mg are also displayed along with those of the moving mass. Deflections of the shaft, V/V_s. W/V_s increase while the Rayleigh coefficient increases as expected in both Figs. 2 and 3. The maximum deflections V/V_s and W/V_s caused by the moving force and those by the moving mass are close to each other in Fig. 2. The main discrepancy between them is that the deflection W/V_s under the mass shifts obviously toward later

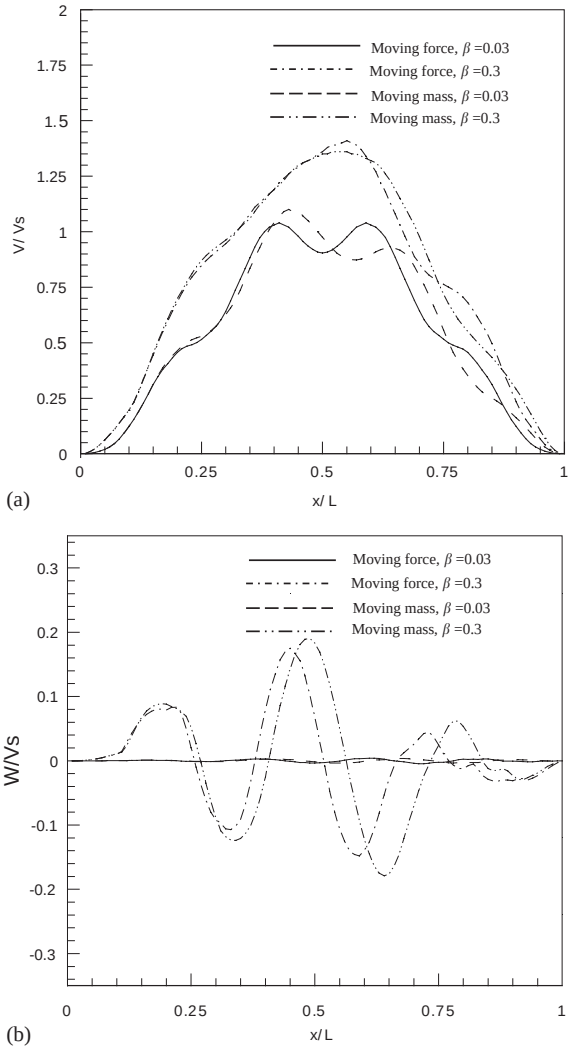

Fig. 2. Normalized deflections under the moving mass and the equivalent moving force for $\bar{\Omega} = 2.5, \bar{m} = 0.2$, $\alpha = 0.1$ and various Rayleigh coefficients. (a) V/V_s, (b) W/V_s.

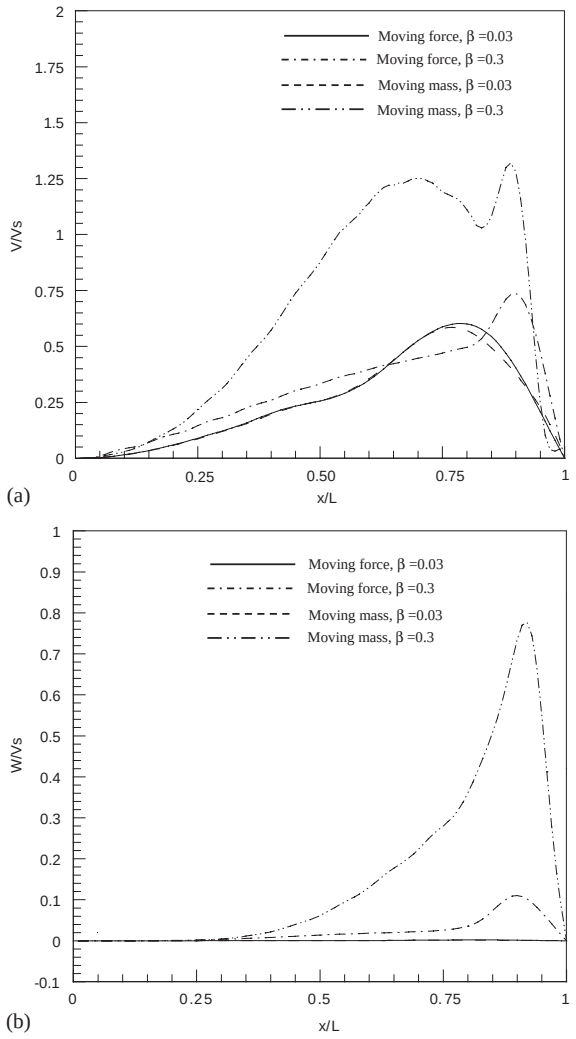

Fig. 3. Normalized deflections under the moving mass and the equivalent moving force for $\bar{\Omega} = 2.5, \bar{m} = 0.2$, $\alpha = 1.5$ and various Rayleigh coefficients. (a) V/V_s, (b) W/V_s.

part of the beam. However, with an increase of either the force or the mass travelling speed, both deflections, V/V_s and W/V_s, will move toward to the later part of the prescribed motion. The deflection W/V_s occurs because of the gyroscopic effect and becomes large mainly due to a higher rotational speed $\bar{\Omega}$ and a large Rayleigh coefficient. The inertia force caused by the moving mass enhances the couplings between the transverse shear and the gyroscopic effect and that between transverse shear and the rotary inertia. In order to quantify the difference in the estimation of the deflection caused by the moving mass and the equivalent moving force, the maximum deflections with respect to two transverse axes are also listed Tables 1–4. Notice that the numerical results for the deflection under the moving force agree well with reported results by Katz [9] and Lee [11]. One can find that the rotational speed has little effect on the spindle vibration response because

Table 1
Maximum normalized deflections V/V_s under the moving force

α	$\bar{\Omega}=0,\ \beta=0.03$	$\bar{\Omega}=0,\ \beta=0.15$	$\bar{\Omega}=0,\ \beta=0.3$	$\bar{\Omega}=2.5,\ \beta=0.03$	$\bar{\Omega}=2.5,\ \beta=0.15$	$\bar{\Omega}=2.5,\ \beta=0.3$
0.11	1.039	1.149	1.471	1.039	1.133	1.405
0.5	1.602	1.717	1.940	1.602	1.704	1.863
1.5	0.603	0.637	0.764	0.603	0.634	0.737

Table 2
Maximum normalized deflections V/V_s under the moving mass, $\bar{m}=0.2$

α	$\bar{\Omega}=0,\ \beta=0.03$	$\bar{\Omega}=0,\ \beta=0.15$	$\bar{\Omega}=0,\ \beta=0.3$	$\bar{\Omega}=2.5,\ \beta=0.03$	$\bar{\Omega}=2.5,\ \beta=0.15$	$\bar{\Omega}=2.5,\ \beta=0.3$
0.11	1.095	1.205	1.517	1.095	1.189	1.361
0.5	1.593	1.684	1.925	1.593	1.675	1.862
1.5	0.585	0.699	1.587	0.585	0.695	1.322

Table 3
Maximum normalized deflections W/V_s under the moving force

α	$\bar{\Omega}=0,\ \beta=0.03$	$\bar{\Omega}=0,\ \beta=0.15$	$\bar{\Omega}=0,\ \beta=0.3$	$\bar{\Omega}=2.5,\ \beta=0.03$	$\bar{\Omega}=2.5,\ \beta=0.15$	$\bar{\Omega}=2.5,\ \beta=0.3$
0.11	0	0	0	0.004	0.080	0.175
0.5	0	0	0	0.005	0.131	0.357
1.5	0	0	0	0.002	0.042	0.110

Table 4
Maximum normalized deflections W/V_s under the moving mass, $\bar{m}=0.2$

α	$\bar{\Omega}=0,\ \beta=0.03$	$\bar{\Omega}=0,\ \beta=0.15$	$\bar{\Omega}=0,\ \beta=0.3$	$\bar{\Omega}=2.5,\ \beta=0.03$	$\bar{\Omega}=2.5,\ \beta=0.15$	$\bar{\Omega}=2.5,\ \beta=0.3$
0.11	0	0	0	0.004	0.075	0.190
0.5	0	0	0	0.005	0.113	0.339
1.5	0	0	0	0.002	0.051	0.777

the nut simulated as a moving mass does not rotate with the spindle. However, for a beam with $\beta=0.3$ and the mass travelling speed $\alpha=1.5$, the maximum deflection is $W/V_s=0.78$, as shown in Fig. 3(b) and in Table 4, which is seven times larger than $W/V_s=0.11$ under the equivalent force listed in Table 4.

4.2. Influences of moving mass size on the shaft response

Fig. 4 shows the normalized deflections V/V_s and W/V_s of a shaft with $\beta=0.15$, rotating at a speed $\bar{\Omega}=2.5$, under the action of a moving mass $\bar{m}=0.2$ and $\bar{m}=0.4$, respectively. Likewise Fig. 5 also displays the same beam subjected to an equivalent moving force with a speed $\alpha=1.5$. Note that both V/V_s and W/V_s are changeless for the moving force, because the deflection is normalized with respective to the static deflection at midspan caused by the force equivalent to the

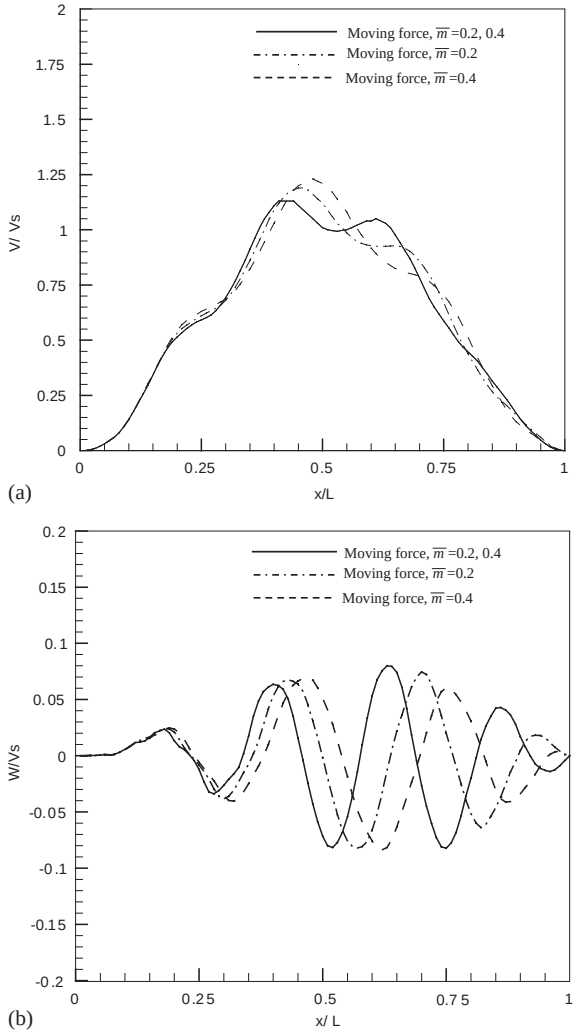

Fig. 4. Normalized deflections under the moving mass and the equivalent moving force for $\bar{\Omega} = 2.5$, $\alpha = 0.1$, $\beta = 0.15$ and various mass ratios. (a) V/V_s, (b) W/V_s.

moving mass. Discrepancies in the deflection between the moving mass and the moving force increase when the moving mass becomes large as expected. Moreover, the deflection under the moving mass shifts toward later part of the beam as the mass ratio increases. One can easily predict that the maximum values of V/V_s and W/V_s increase for a greater moving mass due to high inertia effect. Nevertheless, doubling the moving mass size raises more than two times of the maximum value of W/V_s and obviously the inertia effect influences W/V_s more than V/V_s.

4.3. Influences of moving mass on the critical speeds

A rapid transition of a rotating shaft through a critical speed is expected to limit the whirl amplitudes. Therefore a correct prediction of the critical speed is crucial in determining the

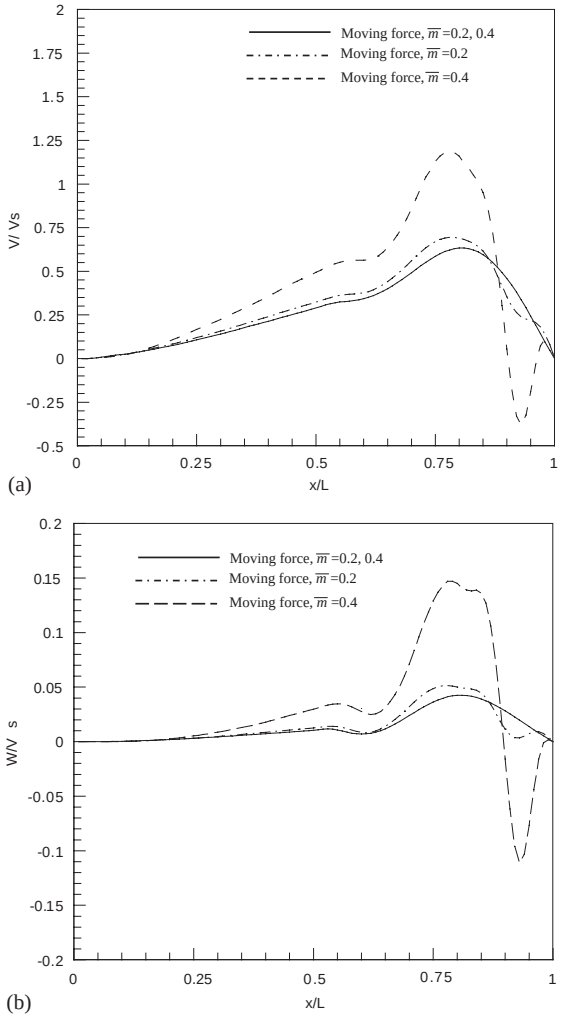

Fig. 5. Normalized deflections under the moving mass and the equivalent moving force for $\bar{\Omega} = 2.5$, $\alpha = 1.5$, $\beta = 0.15$ and various mass ratios. (a) V/V_s, (b) W/V_s.

vibration characteristics of a shaft in a design phase. The critical speeds for rotating shafts with $\beta = 0.03$ and $\beta = 0.3$ are plotted in Figs. 6 and 7, respectively, while the mass located at the midspan is moving at a speed $\alpha = 0.1$. The critical speeds derived from a shaft model with shear deformation included decrease as β increases. The critical speed corresponding to the nth flexural mode of the rotating Timoshenko shaft model is given by [19]

$$(n\pi)^4 + 2an^2\beta^2c^2 - (\delta+1)a^2n^2\beta^2c^2 - a^2c^2 - 2\delta a^3\left(\frac{\beta}{\pi}\right)^4 c^4 + \delta a^4\left(\frac{\beta}{\pi}\right)^4 c^4 = 0, \tag{20}$$

where $\delta = 2(1+\mu)/\kappa$, $c = \Omega/\sqrt{EI/\rho AL^4}$, $a = \omega_n/\Omega$ and μ is the Poisson ratio. If the shear deformation of the rotating shaft is taken into account but the coupling effects induced by the

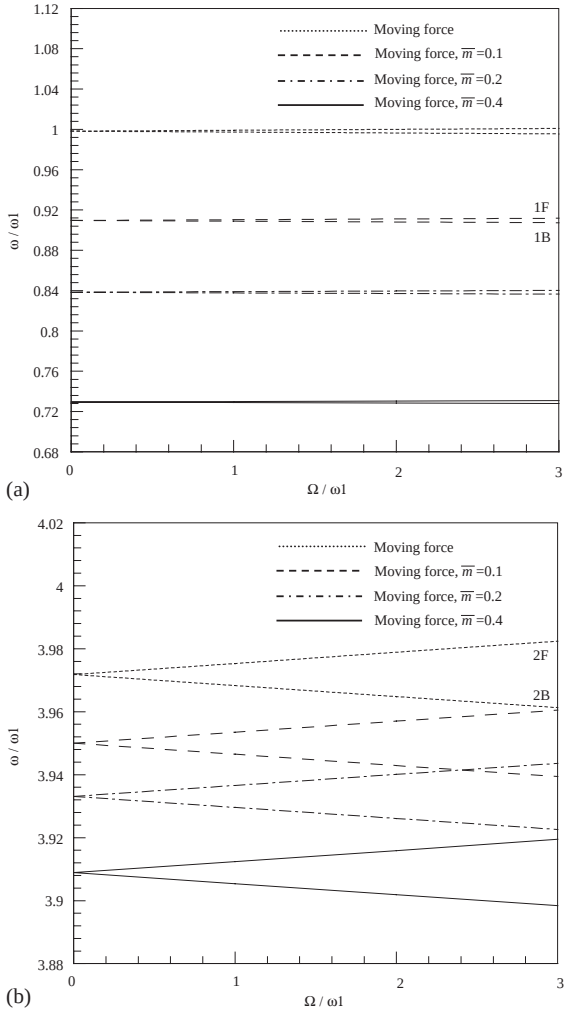

Fig. 6. Normalized forward and backward frequencies for a rotating shaft under the moving mass and the equivalent moving force at $x/L = 0.5$ for $\alpha = 0.1$, $\beta = 0.03$ and various mass ratios. (a) The first critical frequency, (b) the second critical frequency.

shear deformation; such as the coupling between transverse shear and the gyroscopic effects and the coupling between transverse shear and the rotary inertia is neglected, Eq. (20) can be simplified as

$$(n\pi)^4 + 2an^2\beta^2c^2 - (\delta + 1)a^2n^2\beta^2c^2 - a^2c^2 = 0. \tag{21}$$

Then the critical speed corresponding to the nth flexural mode can be obtained analytically as

$$ac = \frac{n^2\beta^2c \pm \sqrt{n^4\beta^4c^2 + n^4\pi^4\left[(\delta + 1)n^2\beta^2 + 1\right]}}{(\delta + 1)n^2\beta^2 + 1}. \tag{22}$$

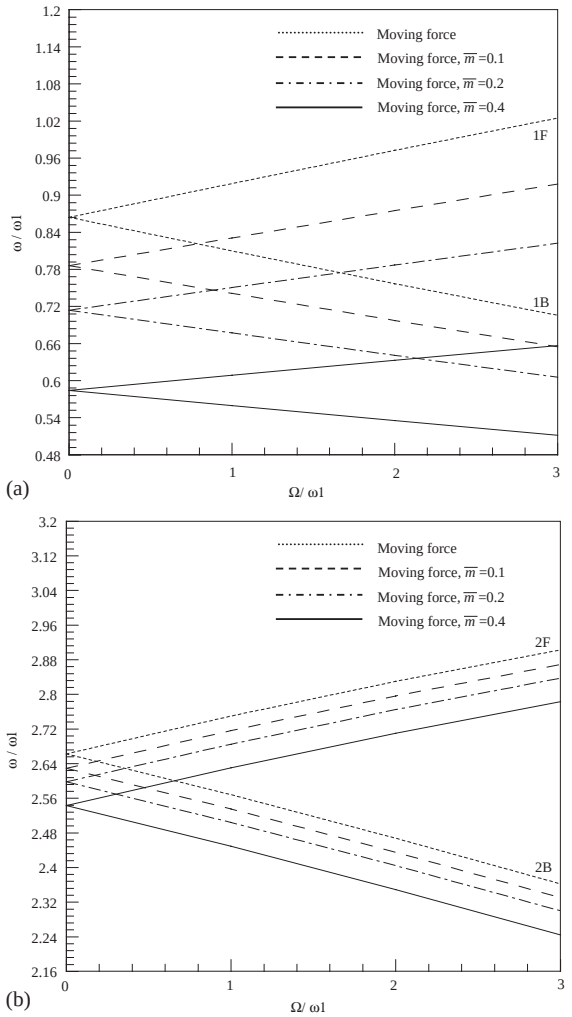

Fig. 7. Normalized forward and backward frequencies for a rotating shaft under the moving mass and the equivalent moving force at $x/L = 0.5$ for $\alpha = 0.1$, $\beta = 0.3$ and various mass ratios. (a) The first critical frequency, (b) the second critical frequency.

Note that $a = 1$, the rotational speed c is equal to $(n\pi)^2$ times the natural frequency ω_n which corresponds to the nth flexural mode of the shaft. When $\beta < 1$ as occurs in most engineering application, Eq. (22) can be furthermore approximated as

$$\frac{ac}{(n\pi)^2} = \frac{(\beta/\pi)^2 c}{(\delta+1)n^2\beta^2+1} \pm \frac{1}{\sqrt{(\delta+1)n^2\beta^2+1}}. \tag{23}$$

Eq. (23) clearly shows that the critical speed decreases as β increases and the critical speed varies much rapidly for a large β when the rotational speed increases. These behaviors are the same for the shaft with a moving mass as seen in Figs. 6 and 7 although the critical speed

calculated using Eq. (23) excludes the effect caused by the moving load. The trends of critical speeds corresponding to different flexural modes are similar to each other and the critical speeds are smaller under the action of moving mass compared to those under the equivalent force. In other words, the critical speeds of the spindle could be seriously overestimated if the ball screw system is modelled either as a shaft subjected to a moving force or as a shaft alone without a moving nut.

5. Conclusions

The dynamic response of a high-speed spindle subject to a high-speed moving mass is studied. Dynamic equations of the system and the corresponding transient response are obtained using Lagrangian approach and Runge–Kutta method, respectively. Influences of parameters on responses of the system such as the mass moving velocity, the Rayleigh coefficient and the mass ratio are discussed. The vibration response of a beam subjected to a moving mass is larger than an equivalent moving force when the Rayleigh coefficient, the mass moving speed and the mass ratio increase as expected. The inertia force caused by the moving mass enhances the couplings between transverse shear and the gyroscopic effect. As a result, for a beam with large Rayleigh coefficient the maximum deflection under the moving mass is larger than a beam under an equivalent force, especially in the orthogonal direction of the moving mass. Moreover, the critical speed of a ball screw could be seriously overestimated if the ball screw system is modelled either as a shaft subjected to a moving force or as a shaft alone without the moving nut.

Acknowledgements

This work was partially supported by the National Science Council of Taiwan, Republic of China under Contract No. NSC 90-2622-E-194-003.

Appendix

The equations of motion for a short and stubby rotating shaft subjected to a moving mass are derived using Hamilton's principle and are expressed as follows:

$$\left(EI - \frac{MV_m^2 EI}{\kappa GA}\delta(x - V_m t)\right)\frac{\partial^4 V}{\partial x^4} + MV_m^2\delta(x - V_m t)\frac{\partial^2 V}{\partial x^2}$$
$$+ \left(-\frac{EI\rho}{\kappa G} - \rho I + \frac{MEI}{\kappa GA}\delta(x - V_m t) - \frac{MV_m^2\rho I}{\kappa GA}\delta(x - V_m t)\right)\frac{\partial^4 V}{\partial x^2 \partial t^2}$$
$$+ (\rho A + M\delta(x - V_m t))\frac{\partial^2 V}{\partial t^2} + \left(\frac{2\Omega\rho^2 I}{\kappa G} + 2\Omega\,\frac{\rho IM}{\kappa GA}\delta(x - V_m t)\right)\frac{\partial^3 W}{\partial t^3}$$

$$+\left(\frac{\rho^2 I}{\kappa G}+\frac{\rho I M}{\kappa G A}\,\delta(x-V_m t)\right)\frac{\partial^4 V}{\partial t^4}-2\Omega\left(\left(\rho I-\frac{M V_m^2 \rho I}{\kappa G A}\delta(x-V_m t)\right)\frac{\partial^3 W}{\partial x^2 \partial t}\right)$$
$$+2MV_m\left(\frac{\partial^2 V}{\partial x \partial t}+\frac{\rho I}{\kappa G A}\,\frac{\partial^4 V}{\partial x \partial t^3}-\frac{EI}{\kappa G A}\,\frac{\partial^4 V}{\partial x^3 \partial t}+\frac{2\Omega \rho I}{\kappa G A}\,\frac{\partial^3 W}{\partial x \partial t^2}\right)\delta(x-V_m t)=f(x,t), \quad \text{(A1)}$$

where the shaft has a cross-sectional area A, second moment of area I, cross-sectional shape factor κ, Young's modulus E, shear modulus G and density ρ. The deformed beam is described by the transverse translations $V(x,t)$ and $W(x,t)$ in the y and z directions, respectively. Notice that the above equation is derived for y co-ordinate. Similarly, one can derive the equation of motion for the z co-ordinate and combine them into a single equation using complex notation. If $M=0$, the equation of motion shown above is reduced to a rotating shaft based on Timoshenko beam model without a moving mass. The equation of motion is obviously complicated. Nevertheless, the equation of motion denotes the force equilibrium and each term represents a distributed force caused by the transverse shear, the gyroscopic effect, the lateral inertia, the rotary inertia and couplings induced from the moving mass. The couplings arising from the moving mass can be assorted as follows:

A. The moving mass inertia that enhances couplings between transverse shear, rotary inertia and the gyroscopic effects is represented by

$$\left(\frac{2\Omega \rho I M V_m^2}{\kappa G A}\,\frac{\partial^3 W}{\partial x^2 \partial t}+\frac{4\Omega \rho I M V_m}{\kappa G A}\,\frac{\partial^3 W}{\partial x \partial t^2}+\frac{2\Omega M \rho I}{\kappa G A}\,\frac{\partial^3 W}{\partial t^3}\right)\delta(x-V_m t). \quad \text{(A2)}$$

B. The moving mass that enhances couplings between transverse shear and the rotary inertia is represented by

$$\left(\frac{M \rho I}{\kappa G A}\,\frac{\partial^4 V}{\partial t^4}+\frac{2MV_m \rho I}{\kappa G A}\,\frac{\partial^4 V}{\partial x \partial t^3}-\frac{MV_m^2 \rho I}{\kappa G A}\,\frac{\partial^4 V}{\partial x^2 \partial t^2}\right)\delta(x-V_m t). \quad \text{(A3)}$$

C. The moving mass that enhances the transverse shear is represented by

$$\left(-\frac{MV_m^2 EI}{\kappa G A}\,\frac{\partial^4 V}{\partial x^4}-\frac{2MV_m EI}{\kappa G A}\,\frac{\partial^4 V}{\partial x^3 \partial t}+\frac{MEI}{\kappa G A}\,\frac{\partial^4 V}{\partial x^2 \partial t^2}\right)\delta(x-V_m t). \quad \text{(A4)}$$

D. The moving mass that enhances the lateral inertia effect is represented by

$$\left(2MV_m\,\frac{\partial^2 V}{\partial x \partial t}+M\,\frac{\partial^2 V}{\partial t^2}+MV_m^2\,\frac{\partial^2 V}{\partial x^2}\right)\delta(x-V_m t). \quad \text{(A5)}$$

References

[1] C.R. Steele, The finite beam with a moving load, *American Society of Mechanical Engineers Journal of Applied Mechanics* 34 (1967) 111–118.

[2] H.D. Nelson, R.A. Conover, Dynamic stability of a beam carrying moving masses, *American Society of Mechanical Engineers Journal of Applied Mechanics* 38 (1971) 1003–1006.

[3] L. Fryba, *Vibration of Solids and Structures Under Moving Loads*, Noordhoff International, Groningen, Netherlands, 1972.
[4] W. Weaver Jr., S.P. Timoshenko, D.H. Young, *Vibration Problem in Engineering*, 5th Edition, Wiley, New York, 1990.
[5] R. Katz, C.W. Lee, A.G. Ulsoy, R.A. Scott, Dynamic stability and response of a beam subject to a deflection dependent moving load, *American Society of Mechanical Engineers Journal of Vibration and Acoustics, Stress and Reliability in Design* 109 (1987) 361–365.
[6] H.P. Lee, The dynamic response of a Timoshenko beam subjected to a moving mass, *Journal of Sound and Vibration* 198 (2) (1996) 249–256.
[7] S. Mackertich, The response of an elastically supported infinite Timoshenko beam to a moving vibrating mass, *Journal of Acoustical Society of America* 101 (1) (1996) 337–340.
[8] H.P. Lee, Dynamic response of a Timoshenko beam on a Winkler foundation subjected to a moving mass, *Applied Acoustics* 55 (3) (1998) 203–215.
[9] R. Katz, C.W. Lee, A.G. Ulsoy, R.A. Scott, The dynamic response of a rotating shaft subject to a moving load, *Journal of Sound and Vibration* 122 (1) (1988) 131–148.
[10] A. Argento, R.A. Scott, Dynamic response of a rotating beam subjected to an accelerating distributed surface force, *Journal of Sound and Vibration* 157 (2) (1992) 221–231.
[11] H.P. Lee, Dynamic response of a rotating Timoshenko shaft subject to axial forces and moving loads, *Journal of Sound and Vibration* 181 (1) (1995) 169–177.
[12] A. Argento, A spinning beam subjected to moving deflection dependent load, Part I: response and resonance, *Journal of Sound and Vibration* 182 (4) (1995) 595–615.
[13] A. Argento, H.L. Morano, A spinning beam subjected to moving deflection dependent load, Part II: parametric resonance, *Journal of Sound and Vibration* 182 (4) (1995) 617–622.
[14] Y.M. Huang, K.K. Chang, Stability analysis of a rotating beam under a moving motion-dependent force, *Journal of Sound and Vibration* 202 (3) (1997) 427–437.
[15] J.W.Z. Zu, R.P.S. Han, Dynamic response of a spinning Timoshenko beam with general boundary conditions and subject to a moving load, *American Society of Mechanical Engineers Journal of Applied Mechanics* 61 (1994) 152–160.
[16] R.P.S. Han, J.W.Z. Zu, Modal analysis of rotating shafts: a body-fixed axis formulation approach, *Journal of Sound and Vibration* 156 (1) (1992) 1–16.
[17] W.T. Thomson, M.D. Dahleh, *Theory of Vibration with Applications*, 5th Edition, Prentice-Hall, Englewood Cliffs, NJ, 1993.
[18] W.H. Enright, J.D. Pryce, Two FORTRAN packages for assessing initial value methods, *ACM Transactions on Mathematical Software* 13 (1987) 1–22.
[19] C.W. Lee, *Vibration Analysis of Rotors*, Kluwer Academic Publishers, Dordrecht, Netherlands, 1993.